Hindawi Publishing Corporation
Advances in Meteorology
Volume 2016, Article ID 4587687, 14 pages
http://dx.doi.org/10.1155/2016/4587687

Research Article

Spatial and Temporal Soil Moisture Variations over China from Simulations and Observations

Xin Lai,[1,2] Jun Wen,[2] Sixian Cen,[3] Xi Huang,[4] Hui Tian,[2] and Xiaokang Shi[5]

[1]*College of Atmospheric Sciences, Plateau Atmosphere and Environment Key Laboratory of Sichuan Province, Chengdu University of Information Technology, Chengdu, Sichuan 610225, China*
[2]*Key Laboratory of Land Surface Process and Climate Change in Cold and Arid Regions, Cold and Arid Regions Environmental and Engineering Research Institute, Chinese Academy of Sciences, Lanzhou, Gansu 730000, China*
[3]*Chengdu Institute of Plateau Meteorology, China Meteorology Administration, Chengdu, Sichuan 610071, China*
[4]*Lijiang Airport Meteorological Station, Lijiang, Yunnan 674100, China*
[5]*Institute of Aeronautical Meteorology and Chemical Deference, Air Force Academy of Equipment, Beijing 100085, China*

Correspondence should be addressed to Jun Wen; jwen@lzb.ac.cn

Received 16 November 2014; Revised 25 May 2015; Accepted 26 May 2015

Academic Editor: Eduardo García-Ortega

The Community Land Model version 4.0 (CLM4.0) driven by the forcing data of Princeton University was used to simulate soil moisture (SM) from 1961 to 2010 over China. The simulated SM was compared to the in situ SM measurements from International Soil Moisture Network over China, National Centers for Environmental Prediction (NCEP) Reanalysis data, a new microwave based multiple-satellite surface SM dataset (SM-MW), and European Centre for Medium-Range Weather Forecasts Interim Reanalysis (ERA Interim/Land) SM data. The results showed that CLM4.0 simulation is capable of capturing characteristics of the spatial and temporal variations of SM. The simulated, NCEP, SM-MW, and ERA Interim/Land SM products are reasonably consistent with each other; based on the simulated SM of summer, it can be concluded that the spatial distribution in every layer was characterized by a gradually increasing pattern from the northwest to southeast. The SM increased from surface layer to deeper layer in general. The variation trends basically showed consistencies at all depths. The simulated SM of summer demonstrated different responses to the precipitation variation. The variation distribution of SM and measured precipitation had consistencies. The humid region significantly responded to precipitation, while the semiarid and arid regions were ranked second.

1. Introduction

Soil moisture (SM) is one of the most important geophysical variables for characterizing the status of the land surface, and it is also an important variable that controls the land-atmosphere interaction. By altering underlying surface variables like soil albedo and soil thermal capacity, changes in SM control the partition of net radiation to sensible heat and latent heat, leading to changes in the water and thermal balances between the lower atmosphere and the land surface. These changes in SM then influence regional climate change [1]. SM spatial and temporal distribution and variations have not only important weather and climate theoretical importance, but also practical importance in the research fields of agriculture, ecology, and economy.

Despite the greater focus being directed to the effects of SM on weather forecasts and climate predictions, the lack of observations with long temporal continuity and high spatial resolution hinders the research on SM characteristics and climatic effects [2]. There are few SM datasets available in the International Soil Moisture Network at present [3–5]. Although the simulation ability of land surface model (LSM) suffers from gaps and uncertainties in forcing data and from model assumptions and generalizations, SM obtained through LSM simulation has good temporal frequency and spatial distribution. Land model especially has very good

physical conception of moisture transport, so it is widely used in research of surface variables like SM [1, 6–9].

Qian et al. [10] evaluated historical simulations of Community Land Model version 3.0 (CLM3) using available observations of SM. The results showed that observed SM variations over Illinois (USA) and parts of Eurasia are generally simulated well, with the dominant influence coming from precipitation. By running the Community Land Model (CLM3.5) over China from 1993 to 2002 using the reanalysis-based precipitation and air temperature and in situ observations in the meteorological forcing dataset, Wang and Zeng [6] discussed the effects of the quality of meteorological forcing data (such as precipitation and temperature) on the simulations of variables in the land surface water cycle. Compared to the in situ measured SM data, the CLM3.5 simulation can generally capture the spatial and seasonal variations of SM but overestimate SM in northeast and east China and underestimate SM in northwest China. Li et al. [1] generated an atmospheric field (ObsFC) for the Community Land Model version 3.5 (CLM3.5) with the support from ground station observations, and SM was simulated over China from 1951 to 2008. The resulting SM indicated that CLM3.5/ObsFC is capable of reproducing the spatial-temporal characteristics and long-term variation trends of SM over China. Using an in situ observation-based forcing field improves the simulation of SM. Guo et al. [11] applied the Variable Infiltration Capacity (VIC) distributed hydrological model [12] with $9 \times 9\,\mathrm{km}^2$ grid resolution and calibrated in the Hanjiang basin. Validation results show that the VIC model can simulate runoff hydrograph with high model efficiency and low relative error. Decharme et al. [13] study the evaluation of a new land surface hydrology within the Noah-WRF land-atmosphere-coupled mesoscale model over the Sahel. An appreciable improvement of the model results is found when the new hydrology is used. The ECMWF Interim Reanalysis (ERA-Interim) [14] and the National Aeronautics and Space Administration (NASA) Modern-Era Retrospective Analysis for Research and Applications (MERRA) [15] provide global reanalyses for the past three decades (from 1979 onward) at high spatial resolution and with modern data assimilation and modeling systems. ECMWF recently developed ERA-Interim/Land simulations, where the ERA-Interim near-surface meteorological forcing is used with the latest version of the ECMWF land surface model [7]. An enhanced MERRA data product, MERRA-Land, has recently been released [9]. Albergel et al. [16, 17] evaluate reanalyses SM products from ERA-Interim, ERA-Interim/Land, and MERRA-Land with global ground-based in situ observations. The three analyses show good skills in capturing surface SM variability.

Besides using modeling approaches, global SM can be estimated through active and passive satellite microwave remote sensing with adequate spatial-temporal resolution and accuracy. Several quasiglobal SM datasets have been generated during the last decade based on either active or passive microwave satellite observations from Advanced Microwave Scanning Radiometer-EOS (AMSR-E) [18, 19], European Remote Sensing Satellite (ERS-1 and ERS-2), MetOp Advanced Scatterometer (ASCAT) [20], Scanning Multichannel Microwave Radiometer (SMMR), Special Sensor Microwave Imager (SSM/I), Tropical Rainfall Measuring Mission (TRMM) Microwave Imager (TMI), WindSat [21, 22], and Soil Moisture and Ocean Salinity mission (SMOS) [23, 24]. The combination/ensemble of these sensors opens up the possibility of studying the global behavior of SM from 1979 onward using only observations [25]. Recently, the first multidecadal satellite-based global SM record has been available [26]. The new consistent global SM data record based on active and passive microwave sensors (SM-MW) has been generated by homogenizing different existing SM products [26–28].

The above research showed that the LSM can reasonably reflect the temporal and spatial distribution of surface variables like SM and soil temperature. As the limitation of available observation datasets, the previous investigations of CLM based on the observation have focused on a single site or small scale, and the simulating period is short. So it is difficult to fully reflect the ability of CLM simulation, and the SM datasets of CLM simulation could not be used in the research of regional SM climatology under the background of climate change. Furthermore, the researches on discussing the response of SM to climate change over China are not well presented. As one of the well-developed land models in the world, the newly released CLM4.0 improves the hydrology scheme of CLM3.5 and depicts the SM dynamic scheme more accurate, it is potential in SM simulation at a continental scale.

In this paper, the CLM4.0 driven by the atmospheric forcing data of Princeton University was deployed to simulate SM spatial distribution and temporal spatial variation from 1961 to 2010 over China. The simulated SM was compared to the ground observations, NCEP Reanalysis data, and SM-MW and ERA Interim/Land SM data. It is expected that all these aspects will provide a full realization of CLM simulation ability over China. Furthermore, the spatial and temporal variations of SM and its response to climate change over China during 1961–2010 will be explored, the shortage of CLM4.0 simulation over China will be summarized and discussed, and the future improvements of the scheme will be prospected.

2. Model and Data

2.1. Introduction of CLM4.0. Community land model (CLM) is one of the most well-developed land surface process models and has the biggest potential development in the world [29]. It integrates advantages of the relative mature process description of Biosphere-Atmosphere Transfer Scheme (BATS), LSM which was established at the Institute of Atmospheric Physics, Chinese Academy of Sciences in 1994 (IAP94), LSM of NCAR, and so forth. It also includes hydrology scheme and parameterization of physical scheme. The CLM is the land model of the Community Earth System Model (CESM) and Community Atmosphere Model (CAM), coupled with many climate models. The model represents several aspects of the land surface including surface heterogeneity and consists of

components or submodels related to land biogeophysics, the hydrologic cycle, biogeochemistry, human dimensions, and ecosystem dynamics. Excessively wet and less variation in SM simulations were recognized as a deficiency of CLM3.5 [30, 31]. The newly released CLM4.0 improved the hydrology scheme of CLM3.5, adopted a modified resolution of the Richards equation, and improved the definition of the lower boundary condition to directly couple the soil water and ground water [31, 32]; CLM4.0 revised soil evaporation parameterization, accounting for the effects of canopy litter and within canopy stability on evaporation [33]. The snow module was significantly improved in CLM4.0 [34–36]. The soil column has been extended to 50 m depth by adding five additional hydrological inactive soil layers [37]. An urban module has been added [38]. The albedo biases were reduced by improving dynamic vegetation functions and patterns [39, 40]. By all above measures, CLM4.0 improved soil water dynamic process in CLM3.5 and leads to reducing the simulated SM and enlarging SM variability. The snow coverage simulated by revised model increased, soil temperatures decreased in organic-rich soils, albedo over the forests and grasslands decreased, and albedo during the transition-season over the snow covered regions increased, all of which are improvements compared to CLM3.5. So, CLM4.0 is selected for this research.

2.2. Data Description

2.2.1. Forcing Data and Land Surface Data in CLM4.0. CLM4.0 was driven by the atmospheric forcing data of Princeton University from 1961 to 2010, with temporal resolution of 3 hours and horizontal resolution of $1^\circ \times 1^\circ$ degrees [41]. The forcing data includes 7 meteorological variables: precipitation, air temperature at 2 m above ground, downward short- and long-wave radiation at surface, surface pressure, specific humidity, and wind speed. The original forcing data is a global, from 1948 to 2010 dataset of meteorological forcing that can be used to drive models of land surface hydrology. The forcing data is a hybrid of data from the NCEP-National Center for Atmospheric Research (NCAR) reanalysis [42] and a suite of global observation based datasets of precipitation, temperature, and radiation. The observation based datasets include Climatic Research Unit (CRU) monthly climate variables, Global Precipitation Climatology Project (GPCP) daily precipitation, TRMM 3-hourly precipitation, and the National Aeronautics and Space Administration (NASA) Langley monthly surface radiation budget. More details of the dataset are described in [41]. The dataset has been used to evaluate the global terrestrial water budget [43] and also to drive the VIC model for exploring global drought characteristics [44]. The land surface datasets released with CLM4.0 were used in this study, which includes topography, soil properties, plant functional types, and land use.

2.2.2. In Situ Measured SM. 30 stations selected from International Soil Moisture Network over China are used to validate CLM4.0 simulation [3–5]. Li et al. [45] used these datasets to verify the ECMWF 40-year Reanalysis (ERA-40) and NCEP Reanalysis data of SM. The datasets were successfully used to verify and explore models [46]. The datasets were converted into volumetric SM and can be conveniently used to evaluate and improve simulations.

2.2.3. NCEP Reanalysis Data. The NCEP Climate Forecast System Reanalysis (CFSR) was completed over the 31-year period of 1979 to 2009 in January 2010. The CFSR was designed and executed as a global, high resolution, coupled atmosphere-ocean-land surface-sea ice system to provide the best estimate of the state of these coupled domains over this period. The CFSR includes (1) coupling of atmosphere and ocean, (2) an interactive sea-ice model, and (3) assimilation of satellite radiances by the gridpoint statistical interpolation scheme over the entire period. The global land surface model has 4 soil levels. Most available in situ and satellite observations were included in the CFSR. Satellite observations were used in radiance form [47]. CFSR land surface output products will serve many purposes, including providing estimates and diagnoses of the earth's climate state, over the satellite data period, for community climate research [47]. The data is distributed via http://rda.ucar.edu/datasets/ds093.2/. In this study, surface SM from CFSR is from the first soil layer (0–10 cm) and has a spatial resolution of 0.5°. The SM data are provided in volumetric units (m^3/m^3).

2.2.4. Remotely Sensed Data. In response to the Global Climate Observing System (GCOS) endorsement of SM as an Essential Climate Variable (ECV), the European Space Agency (ESA) Water Cycle Multi-Mission Observation Strategy (WACMOS) project and Climate Change Initiative (CCI, http://www.esa-soilmoisture-cci.org/) have supported the generation of a SM product based on multiple microwave sources. The first version of the combined product, SM-MW, was released in June 2012 by the Vienna University of Technology. The merged product is the output of blending the active and passive SM products, which are derived from SMMR, SSM/I, TMI, and AMSR-E for the passive datasets and Active Microwave Instrument-Windscat (AMIWS) and MetOp (ASCAT) for the active datasets. This data has been produced following the method described by [26–28]. The homogenized and merged product presents surface SM with a global coverage and a spatial resolution of 0.25°, and the temporal resolution is 1 day with its reference time at 0:00 UTC. The SM data are provided in volumetric units (m^3/m^3). SM-MW was used to evaluate SM products [17, 48].

2.2.5. ERA Interim/Land Reanalysis. ERA-Interim/Land is a global land surface reanalysis dataset covering the period 1979–2010. It describes the evolution of SM, soil temperature, and snowpack. ERA-Interim/Land is the result of a single 32-year simulation with the latest ECMWF land surface model driven by meteorological forcing from the ERA-Interim atmospheric reanalysis. The horizontal resolution is about 80 km and the time frequency is 3 hours. ERA-Interim/Land includes a number of parameterization improvements in

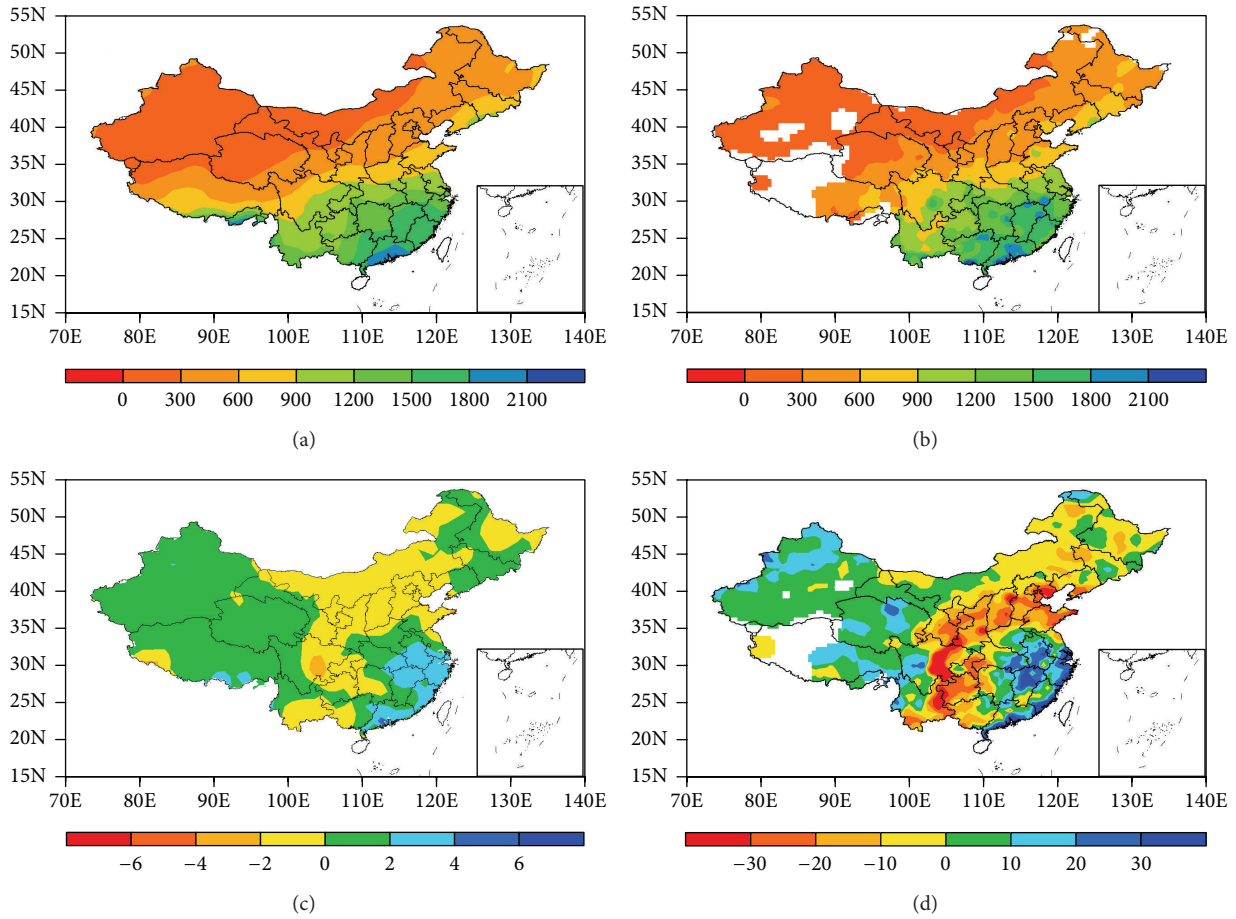

Figure 1: The intercomparison between Princeton precipitation and measured precipitation of 1961–2010. (a) Princeton annual mean precipitation (unit: mm); (b) ground measured annual mean precipitation (unit: mm); (c) Princeton annual precipitation variation linear trend (unit: mm/10 a); and (d) ground measured annual precipitation variation linear trend (unit: mm/10 a).

the land surface scheme with respect to the original ERA-Interim dataset, which makes it more suitable for climate studies involving land water resources. The quality of ERA-Interim/Land is assessed by comparing with ground-based and remote sensing observations [7]. The SM data of ERA-Land product was used to analyze the skill and global trend of SM [17]. In this study, surface SM from ERA Interim/Land is from the first soil layer (0–7 cm).

3. Validation of Simulations

The simulation region of this study is domain of 70°–135°E, 15°–55°N. To stabilize the hydrology process and spin-up CLM model, CLM4.0 was firstly run twice for 1961–2010 simulation years with Princeton forcing data, and, consequently, the simulations of soil water variables were output at a time scale of 1961 to 2010 and horizontal resolution of 0.5°× 0.5°. Firstly, the Princeton forcing data was verified with measured data, and then the simulated SM was compared to the ground observations, NCEP Reanalysis data, and SM-MW and ERA Interim/Land SM data.

3.1. Validation of Forcing Data. Precipitation and temperature are two important variables which influence SM variation. In this paper, precipitation and temperature in Princeton forcing data were validated with ground measured data. The ground measured data is downloaded from China Meteorological Data Sharing Service System of China Meteorological Administration (CMA). Not all stations have long enough time series for climate studies. After screening out unqualified stations, 584 stations for precipitation and 599 stations for temperature from 1961 to 2010 were selected for this study. The precipitation and temperature data were recorded one or several times per day, and they were all converted to daily data. It is to be seen from Figure 1 that Princeton precipitation basically reflects spatial distribution of ground measured precipitation, and precipitation decreased from northwest to southeast. Princeton precipitation also basically reflects spatial distribution of ground measured precipitation variation trends. Precipitation decreased in north of northeast, north China, Inner Mongolia, and parts of the southwest, while precipitation increased in the southeast and south China. But compared to measured precipitation, the absolute value of Princeton precipitation linear trends was small.

From the results of intercomparison between Princeton and ground measured data, it is concluded that the Princeton precipitation and temperature basically reflect spatial distribution and variation trends of measured data. As a result it could be used to drive CLM4.0 to simulate SM over China.

3.2. Comparison of Spatial Distribution between Simulated and Measured SM. The spatial distributions of the simulated and measured SM for April to November were compared because the observations were suspended during frozen period. The spatial distributions of simulated and measured SM were basically consistent with each other as shown in Figure 2. The humid regions were located over the northeast China and Jianghuai basin, and the SM was around 0.25 in the northeast China. Dry region was located over Hetao region, and SM was around 0.15 (Figure 2(b)). The simulated SM reasonably reflected spatial distribution characteristics of measured SM. The spatial distribution of the simulated SM was characterized by a gradually increasing pattern from the northwest to southeast. The spatial pattern of measured SM at 0–50 cm depth was basically consistent with 0–10 cm depth (Figure 2(d)). The measured SM in most stations over northeast China was larger than that at 0–10 cm depth. This result implied that SM in most stations over northeast China increased from shallow depth (0–10 cm) to deep depth (0–50 cm). The spatial distributions of simulated SM in 0–50 cm depth (Figure 2(c)) and measured SM were basically consistent with each other. Simulated SM in 0–50 cm depth is larger than 0–10 cm depth over northwestern, southern area of Yangtze River, and partial areas of southwest China. The spatial distributions of the simulated SM by CLM4.0 were generally consistent with the results of previous studies in China [1]. But the simulated SM was systematically larger than measured SM at two depths. The bias percent (Figures 2(e) and 2(f)) showed that simulated SM was larger than the measured SM at 0–10 cm layer in most stations throughout China. The simulated SM was larger than the measured SM by 60% over Hetao region. Simulated SM was larger than the measured SM in most stations at 0–50 cm layer. Simulated SM was larger than the measured SM in most stations over northeast China. But the stations where simulated SM was larger than measured SM decreased, and bias decreased in most stations. The reason is that measured SM in most stations over northeast China increased from shallow depth (0–10 cm) to deep depth (0–50 cm), simulated SM did not have obvious variations, and bias decreased in most stations.

3.3. Comparison of Temporal Variation between Simulated and Measured SM. Figure 3 showed the linear trends (linear regression coefficient) and bias percent (the percent of bias and in situ, and bias is simulations minus in situ) of simulated SM and measured SM at two different layers (0–10 cm, 0–50 cm) during 1981–1999. The variation trends of measured SM (Figures 3(b) and 3(d)) showed that measured SM mainly decreased in northeast China and Hetao region. Simulated SM (Figures 3(a) and 3(c)) basically reflected variation trends of measured SM. The simulated SM decreased in the northeast China and Hetao region and mainly decreased in the northwest China.

Table 1: The correlation coefficients between simulated monthly mean and measured SM of each layer over the subregions.

Regions	0–10 cm	10–20 cm	20–30 cm	30–50 cm	0–50 cm
R1	0.18*	−0.09	−0.26	−0.34	−0.2
R2	0.43**	0.35**	0.34**	0.3**	0.35**
R3	0.23**	0.23**	0.29**	0.32**	0.3**

*Significant at the 0.05 level; **Significant at the 0.01 level.

With the landscape and referring to Nie et al. [49], the study area is divided into 3 parts (Figure 4) in this study. Region 1 is the subhumid northeast zone. Region 2 is the semiarid Loess Plateau of mountains and hills covered by scrubland and steppe. Region 3 is a main agricultural area of China, with a typical subhumid and temperate climate. The variations of SM were separately discussed in the following parts. Figure 4 showed the interannual variations of simulated monthly mean and measured SM. The left figures represented SM at 0–10 cm depth; the right figures represented SM at 0–50 cm depth. More statistic figures in Figure 4 were listed in Tables 1, 2, and 3. SM values are first averaged across the regions before computing the statistics. Table 1 showed the correlation coefficients between simulated monthly mean and measured SM at each layer over the subregions. Figure 4 showed that simulated SM basically reflected interannual and yearly variations of measured SM except region 1 at 0–50 cm depth; the humid and arid points were matching. Figure 4 together with Table 1 showed that correlation between simulated and measured SM was significant in region 2 and region 3; correlation coefficients of region 2 were most significant. Correlation coefficient of region 1 was significant only at 0–10 cm depth. The interannual variations at 0–50 cm depth of region 1 showed that the simulated SM reflected yearly variations of measured SM, but there was a phase shift compared to measured SM, and this caused the correlation coefficient to be negative. Correlation between simulated and measured SM of region 1 and region 2 decreased when depth increased; this may relate to imperfect hydrological process in CLM4.0. The simulation of SM in surface is better than in deep layer over some regions. The in situ SM measurements are credible. The simulation of CLM4.0 is imperfect, even though it can capture trends of temporal variation. The land surface in northwest China (region 1) is complex, including forest, river, mountain; the simulation in region 1 is not reasonable. So the correlations in region 1 are lowest or negative. Correlations in south China (region 3) are relatively low. SM in region 3 is always humid; variations of simulated SM caused by forcing data could not be perfect. Simulation ability in region 3 could not reach the variation range. Correlations between CLM4.0 and in situ observations are not good in some stations. But the result is acceptable.

Table 2 presented root mean squared errors (RMSE) and bias between simulated monthly mean and measured SM at each layer over the subregions. The results of RMSE and bias showed that simulated SM was systematically larger than

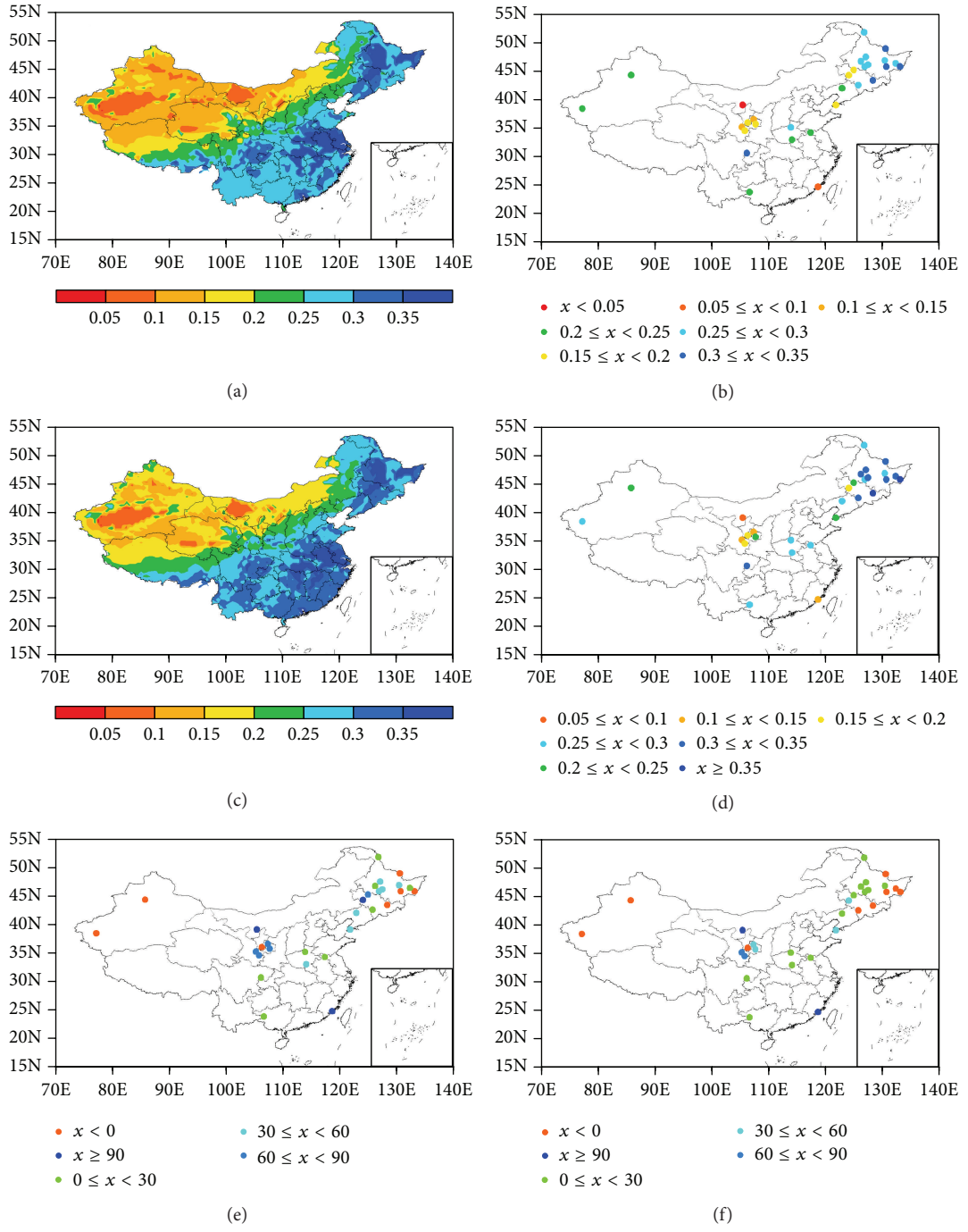

Figure 2: Spatial distribution of the simulated mean and measured SM for April to November of 1981–1999 (unit: m^3/m^3). (a) CLM4.0 simulated SM (0–9.06 cm); (b) measured SM (0–10 cm); (c) CLM4.0 simulated SM (0–49.3 cm); (d) measured SM (0–50 cm); (e) bias percent between CLM4.0 simulated (0–9.06 cm) and measured (0–10 cm) SM; and (f) bias percent between CLM4.0 simulated (0–49.3 cm) and measured (0–50 cm) SM.

Table 2: The RMSE and bias between simulated monthly mean and measured SM of each layer over the subregions (unit: m^3/m^3).

Regions	0–10 cm		10–20 cm		20–30 cm		30–50 cm		0–50 cm	
	RMSE	Bias	RMSE	Bias	RMSE	Bias	RMSE	Bias	RMSE	Bias
R1	0.067	0.062	0.039	0.028	0.032	0.013	0.03	0.004	0.035	0.022
R2	0.09	0.084	0.088	0.081	0.093	0.088	0.1	0.095	0.094	0.09
R3	0.094	0.083	0.068	0.054	0.059	0.045	0.041	0.022	0.057	0.044

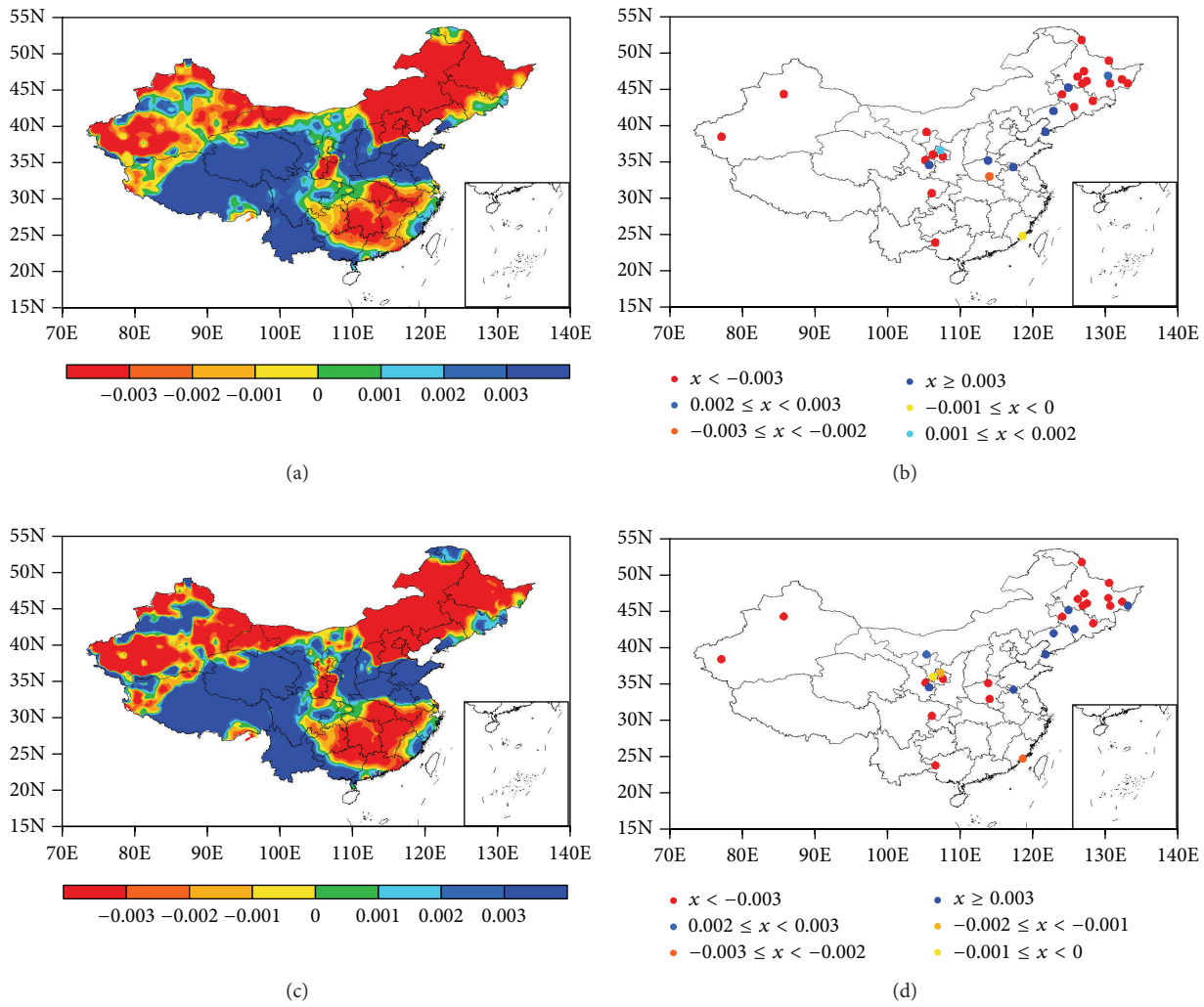

Figure 3: Spatial distribution of variation linear trends of simulated mean and measured SM for April to November of 1981–1999 (unit: $(m^3/m^3)/10$ a). (a) CLM4.0 simulated SM (0–9.06 cm); (b) measured SM (0–10 cm); (c) CLM4.0 simulated SM (0–49.3 cm); and (d) measured SM (0–50 cm).

the ground measured SM at each layer over the three subregions. The RMSE and bias decreased when soil depth increased in region 1 and region 3. In region 1 the measured SM increased when soil depth increased, but variations of simulated SM were not obvious; this made the bias decrease when depth increased. In region 3, the measured SM increased when depth increased, but simulated SM decreased when depth increased; this also made the bias decrease when depth increased.

Table 3 shows the linear trends of simulated and measured SM over the subregions. The linear trends of simulated and measured SM over the three subregions at 0–10 cm depth and 0–50 cm depth were basically consistent at daily, monthly, and yearly time scales. The simulated and measured SM showed decreasing trends of two layers in region 1 and region 2; the simulated and measured SM mostly showed increasing trends of two layers in region 3. The table showed that CLM had good ability to simulate linear trends of different depth and time scales. Simulation of linear trends at 0–10 cm depth was better than 0–50 cm depth; bias was less than that at 0–50 cm depth.

3.4. Comparison between Measured, CLM4.0, NCEP Reanalysis, ERA Interim/Land, and Microwave SM. Figure 5 showed spatial distributions of three kinds of SM products. The spatial distributions of four SM products (CLM4.0, NCEP, ERA Interim/Land, and SM-MW) and measured SM were basically consistent with each other. In general, the four SM products reasonably reflected spatial distribution characteristics of measured SM. The four SM products gradually increased from northwest to southeast. From distribution difference it was revealed that humid regions of CLM4.0 SM were located over northeast China and Jianghuai region

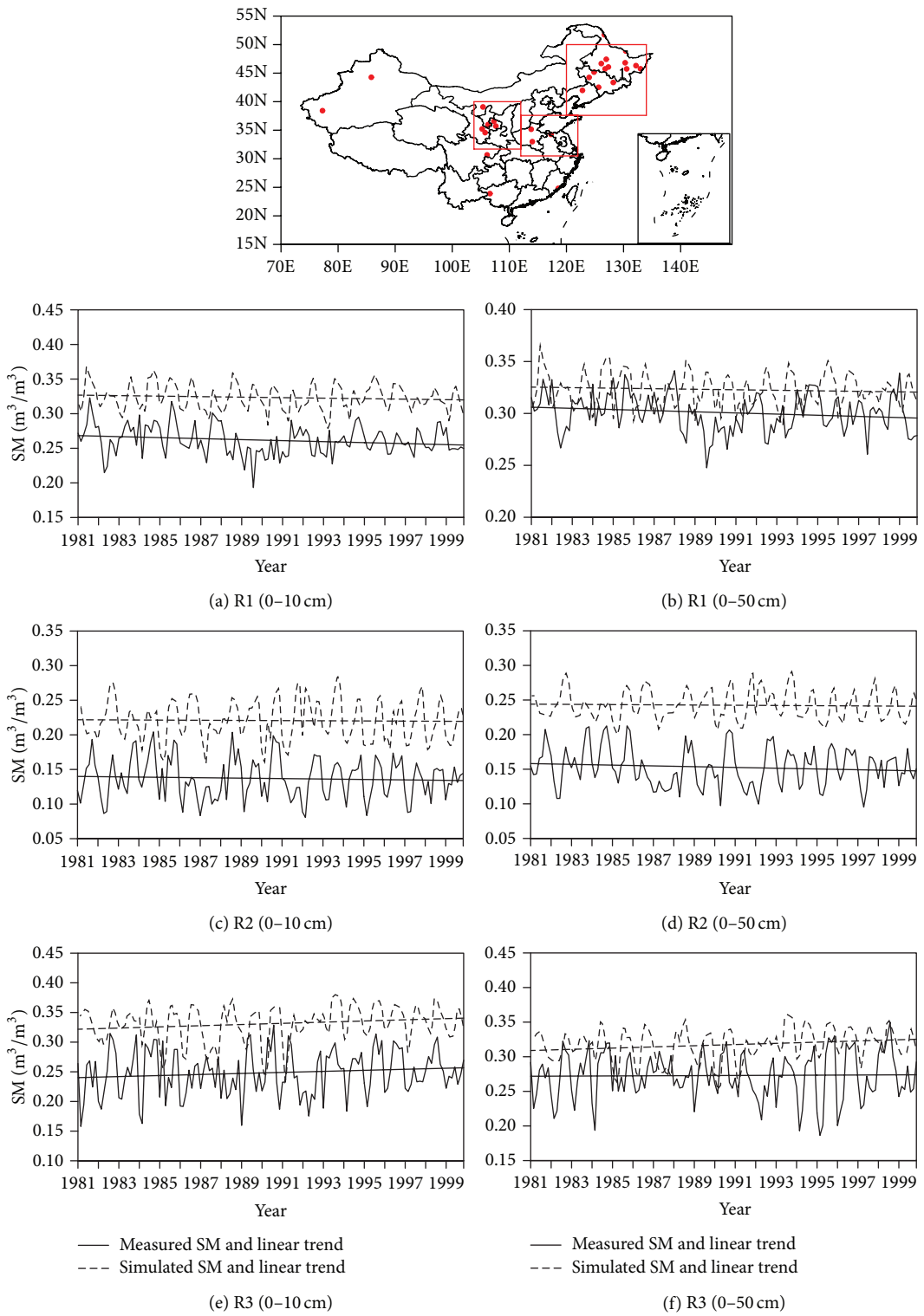

FIGURE 4: The interannual variations of CLM4.0 simulated monthly mean and the ground measured SM for 1, 2, and 3 regions (a, c, and e) 0–10 cm depth; (b, d, and f) 0–50 cm depth.

(Figure 2(a)). The humid regions of NCEP SM were located over the east of the Tibetan Plateau, the middle and lower reaches of Yangtze River, and south China. Humid regions of ERA Interim/Land were located over northeast China, the middle and lower reaches of Yangtze River, and south China. Humid regions of SM-MW were located over southern area of 30°N. Extent of arid regions in northwest China of the four SM products was different from each other.

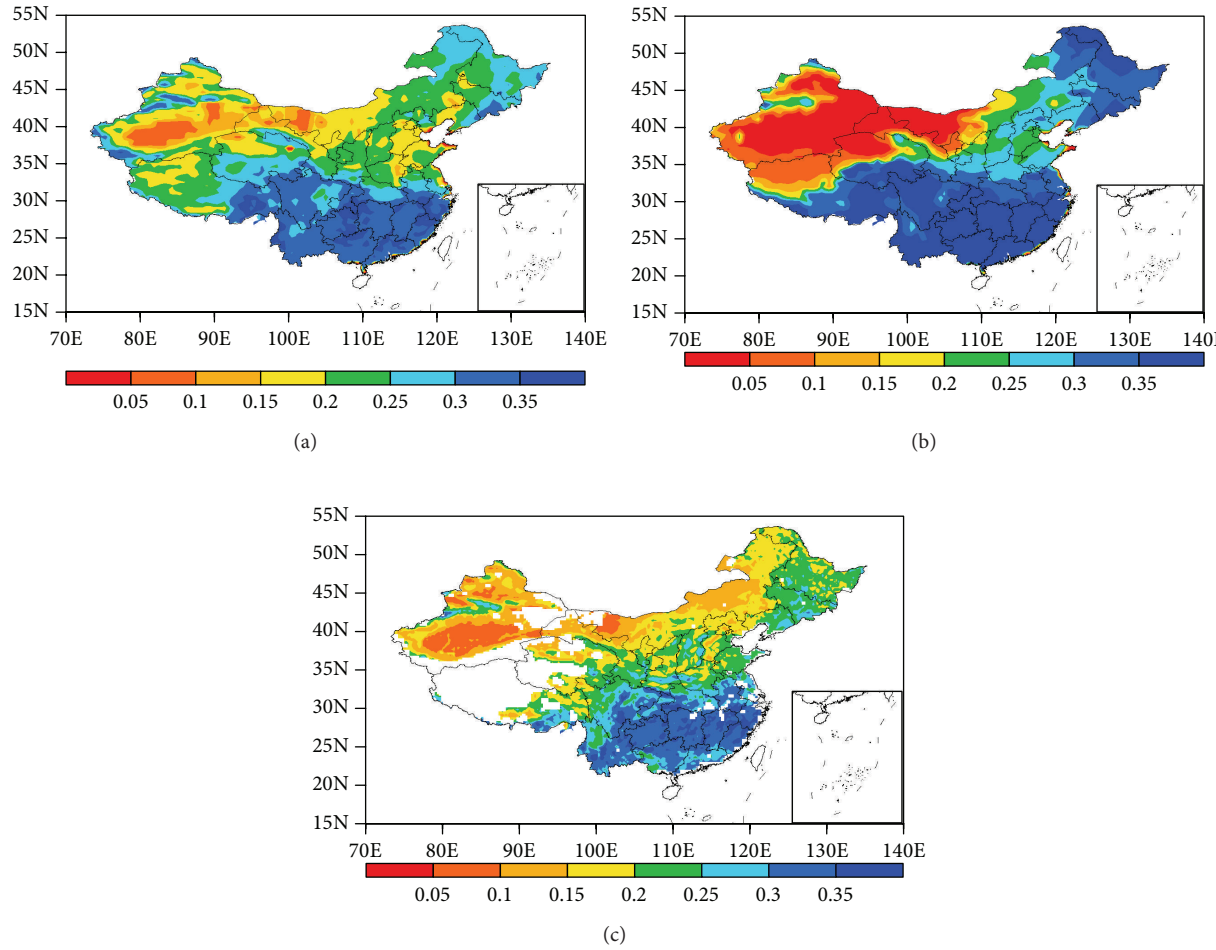

Figure 5: Spatial distribution of SM for April to November of 1981–1999 (unit: m^3/m^3). (a) NCEP SM (0–10 cm); (b) ERA Interim/Land (0–7 cm); and (c) SM-MW.

Table 3: The linear trends of simulated and measured SM over the subregions (unit: $(m^3/m^3)/10$ a).

Regions	0–10 cm		0–50 cm	
	Obs.	Simu.	Obs.	Simu.
Daily				
R1	−0.0072**	−0.0056*	−0.0055**	−0.0032
R2	−0.0031	−0.0015	−0.0055*	−0.0015
R3	0.0088*	0.0096**	0.0012	0.0096**
Monthly				
R1	−0.0072*	−0.0037	−0.0055	−0.0026
R2	−0.0031	−0.0012	−0.0056	−0.0016
R3	0.0088	0.0099	0.0011	0.0086*
Yearly				
R1	−0.0077	−0.0045	−0.0052	−0.0035
R2	−0.0048	−0.0032	−0.0069	−0.003
R3	0.0072	0.0087	−0.0005	0.0076

*Significant at the 0.05 level; **Significant at the 0.01 level, F-test.

4. Temporal Spatial Variation of SM in China and Its Possible Response to Climate Change

Because soil was frozen in the autumn, winter, and early spring of northern areas of China, the summer was chosen as the representative season to investigate the spatial distribution, temporal variation of SM, and its possible response to climate change. The SM spatial distributions of different layers (0–9.06 cm, 9.06–16.56 cm, 16.56–28.92 cm, 28.92–49.3 cm, and 0–49.3 cm) in summer of 1961–2010 were simulated by CLM4.0. In general, the spatial distributions of every soil layer were characterized by a gradually increasing pattern from the northwest to the southeast. Dry regions were located over the Xinjiang, Qinghai, Gansu Province, and the western Inner Mongolia. There are low precipitation and strong radiation in these regions, and average SM was below 0.20 (0–49.3 cm). The most humid regions were located over the Northeast Plain, Jianghuai region, and the Yangtze River

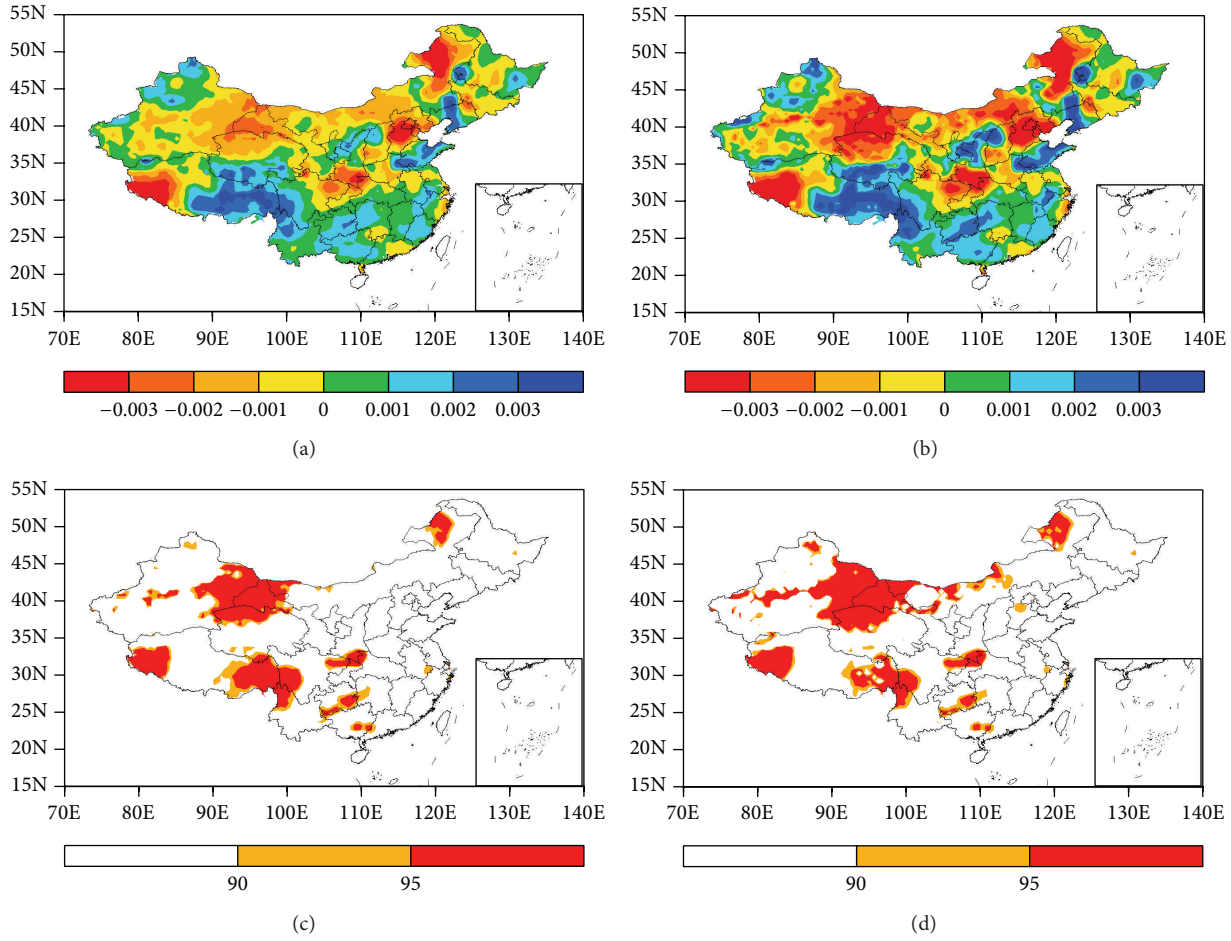

Figure 6: Spatial distribution of simulated mean SM variation linear trends for the summer (June–August) of 1961–2010 (unit: $(m^3/m^3)/10$ a): (a) 0–9.06 cm; (b) 0–49.3 cm and significant level for variation linear trends (unit: %; orange, significant at the 90% level; red, significant at the 95% level; *F*-test): (c) 0–9.06 cm; (d) 0–49.3 cm.

basin. Precipitation in these regions was relatively larger, and average SM exceeded 0.35 (0–49.3 cm). SM increased when soil depth increased in the northwest, southwest, and south China. The increase trend was most obvious at 28.92–49.3 cm depth, and the SM in most areas exceeded 0.30 except part of northwest. The SM increased from surface layer to deeper layer in general. The spatial distributions of simulated SM by CLM4.0 were basically consistent with other works [1].

Figure 6 showed spatial distribution of simulated mean SM variation linear trends for the summer (June–August) of 1961–2010 in two layers. The variation trends basically showed consistencies in all layers. The SM mainly decreased in the northern area of 35°N besides the western Xinjiang Province and partial regions of northeast China, and SM mainly increased in Yangtze River basin, south and southwest China to the southern area of 30°N. Variations were significant in partial region of northwest China in 0–49.3 cm layer, and variations in part region of southwest were significant. The decreasing trends were more significant with soil depth increase in domain north of 35°N arid and semiarid regions, showed arid trends in north regions, and were more severe with soil depth increase. The SM appreciably increased with soil depth increase in south regions, and trends were not significant. Compared to variation trends of Princeton precipitation and temperature of the same time period (1961–2010), it is shown that temperature increased in most regions of China. In northern areas of 35°N, the precipitation increased in Xinjiang province and partial regions of northeast China and decreased in other regions. In southern areas of 35°N, the precipitation increased in Jianghua region, Yangtze River basin, south China, and partial region of southwest China. The variations were basically consistent with measured temperature and precipitation [50]. Under the global warming background, the simulated SM basically demonstrated responses to the precipitation variation. The simulated SM decreased in most regions of north China, the simulated SM increased in Jianghua region, Yangtze River basin, and south China, and the variations were more obvious in deep layer.

Because of the regional heterogeneity of SM variation and its trends to climate change [1] and the fact that SM is very sensitive to precipitation in the forcing datasets [10], the arid region of the northwest, semiarid region of north China, and humid region of the middle and lower reaches of Yangtze

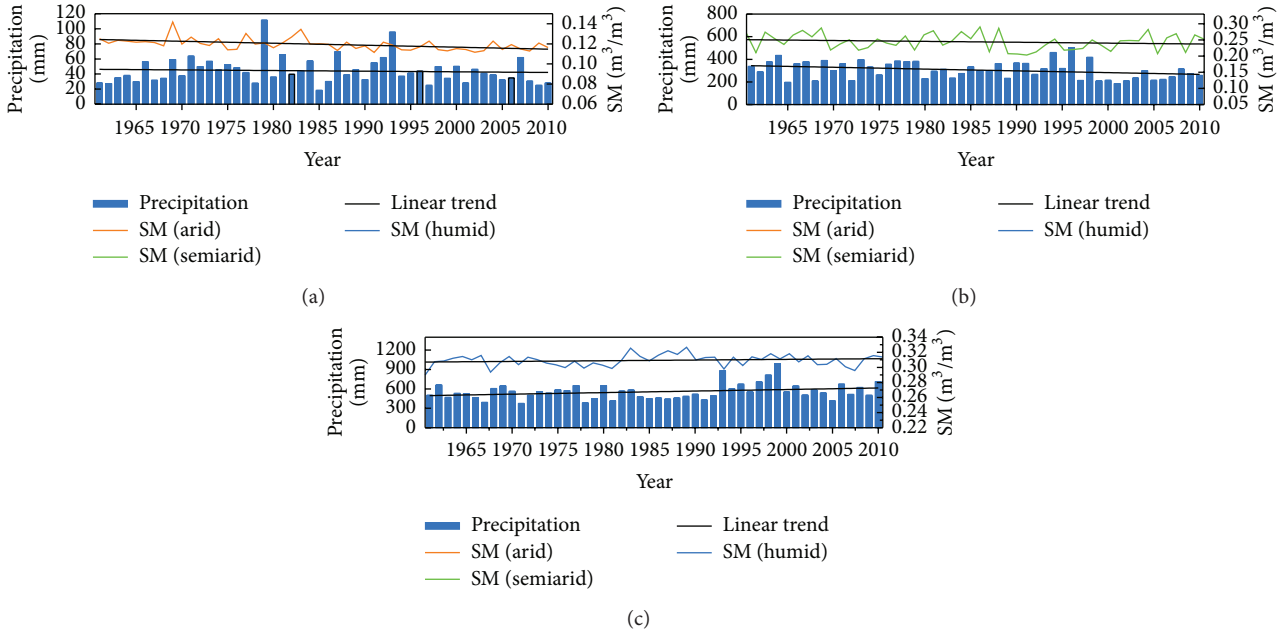

FIGURE 7: Intercomparison of the variation trends between the simulated SM and forcing precipitation in summer (June–August) in typical regions for the period 1961–2010. (a) Arid region; (b) semiarid region; and (c) humid region.

River and the south China were chosen as typical regions in this study to discuss SM variation and regional heterogeneity of its response to precipitation during 1961–2010. Variations in the three regions were somewhat significant. Figure 7 showed intercomparison of variation trends between the simulated SM and forcing precipitation of the summer (June–August) in typical regions for the period 1961–2010. SM in arid region significantly decreased (statistically significant at $\alpha = 0.01$ level, F-test), and precipitation decreased too. SM and precipitation in semiarid region slightly decreased. SM and precipitation in humid region slightly increased. Temperature increased in all the three regions, and increase trends were significant in arid and semiarid regions (figures were not provided). Correlation coefficient of monthly mean SM and precipitation in humid region was 0.47, 0.36 in semiarid region, all were statistically significant at $\alpha = 0.01$ level. Correlation coefficient of monthly mean SM and precipitation in arid region was 0.16 and was statistically significant at $\alpha = 0.05$ level. Precipitation in humid region was large; the influences of evapotranspiration on SM were small because of the high SM in the region. Precipitation was the principal variable that controlled SM in the humid region. SM in semiarid and arid regions is relatively lower; the influence of precipitation was weakened in these regions. The combined actions of climatological factor, surface properties, and additional factors controlled and complicated the variations in SM [1]. To sum up, the simulated SM basically demonstrated responses to the precipitation variation under the global warming background, and correlation coefficients between SM and precipitation were significant positive values; this conclusion was similar to that included in other researches [51]. Precipitation decreased in the arid region of the northwest, semiarid region of the north China, and precipitation increased in humid region of south. The variations were basically consistent with measured precipitation. The simulated SM of summer demonstrated different responses to the precipitation variation. The simulated SM decreased in the arid region of the northwest, semiarid region of the north China, and increased in humid region of south. Response to precipitation was most significant in humid region, while the semiarid and arid regions were ranked second.

5. Discussion

In general, CLM4.0 simulations captured the temporal spatial variation of the measured SM. The spatial distribution of simulated SM is basically consistent with NCEP Reanalysis, SM-MW, and ERA Interim/Land SM data.

5.1. SM Range. The SM numerical simulations are still challengeable at this stage; the simulated results are only potential in actual applications. Results presented in the previous section show that CLM4.0 simulations tend to overestimate SM over China. There are several causes for these discrepancies between simulated and measured SM. The measured SM is taken at a given site, but the spatial distribution of SM is heterogeneous. There is uncertainty in the measured SM at a given depth to represent SM of whole layer. The simulated SM denoted SM at given node to represent SM of whole layer; it also induced uncertainty. Layer depth difference of measurement and simulation also causes errors. Moreover, the simulated SM is average value of grid, the measured SM is value at a given site, and the intercomparisons

have uncertainty. Mismatch between the point measurement and model grid result is not well processed; an up-scaling processing is also needed for ground measurements. At the same time, difference between land surface datasets of CLM4.0 and practical surface datasets of China, imperfect description of hydrological scheme in CLM4.0, and accuracy of atmospheric forcing datasets of the model can make simulation bias. The vertical SM transport is governed by infiltration, surface and subsurface runoff, gradient diffusion, gravity, canopy transpiration through root extraction, and interactions with groundwater, but description of transport of soil heat and SM is not perfect in CLM4.0.

The global land surface datasets of CLM4.0 might not be fully applicable in China. The implementation of new datasets such as the new soil texture, soil color, and plant functional types could lead to better results. A China dataset of soil properties for land surface modeling could be used [52], which is from http://westdc.westgis.ac.cn/data/11573187-fd64-47b1-81a6-0c7c224112a0. Satellite remote sensing can provide high spatial-temporal SM product; its regional distribution is reliable, but the absolute values are still questionable; this is also the case for other reanalysis datasets. In order to overcome these shortages in our future investigations, the improvement of hydrological process modeling, atmospheric forcing datasets, and land surface data is important direction for further development of CLM4.0.

5.2. SM Variability. In this study observations at specific sites are compared with CLM4.0 output at resolution of 0.5°. Spatial variability of SM is very high and can vary from centimeters to meters. Precipitation, evapotranspiration, soil texture, topography, vegetation, and land use could either enhance or reduce the spatial variability of SM depending on how it is distributed and combined with other factors [53]. While comparisons between CLM4.0 simulations and in situ data provide good correlations, they still have high RMSEs as discussed above. These results are in agreement with the suggestion that the true information content of modeled SM does not necessarily rely on their absolute magnitudes but instead on their time variation [54–57]. And their time variation represents the time-integrated impacts of antecedent meteorological forcing on the hydrological state of the soil system with the model [54].

6. Conclusion

The CLM4.0 driven by the atmospheric forcing data of Princeton University was deployed to simulate SM from 1961 to 2010 over China. The simulated SM was compared to the ground observations, NCEP Reanalysis, SM-MW, and ERA Interim/Land SM data. The characteristics of the spatial distribution and temporal spatial variation of SM and its response to climate change were discussed. The following conclusions are drawn.

CLM4.0 simulation was capable of capturing characteristics of the spatial distribution and temporal spatial variation. The simulated SM reasonably reflects spatial distribution characteristics of measure SM, where the humid regions were located over northeast China and Jianghuai basin and dry region was located over Hetao region. But the simulated SM was systematically higher than the observations in each layer over these regions; the simulated SM revealed the measured variation trends of the different layers at different time scales. Correlation between measured and simulated SM was not significant below 10 cm depth in northeast China, and correlation was significant in the other two regions of each layer. The simulated, NCEP, SM-MW, and ERA Interim/Land SM products were reasonably consistent with each other.

Based on the simulated SM of summer (June to August) in 1961–2010, it was concluded that the spatial distribution in every layer was characterized by a gradually increasing pattern from the northwest to southeast. Dry regions were located over the Xinjiang, Qinghai, and Gansu Provinces and the western Inner Mongolia, while the most humid regions were located over the Northeast Plain, Jianghuai region, and the Yangtze River basin. The SM increased from surface layer to deeper layer in general; the variation trends basically showed consistencies in all layers. SM mainly decreased in the northern area of 35°N besides western Xinjiang Province and partial regions of northeast China, and SM mainly increased in Yangtze River basin, south and southwest China in the southern area of 30°N. The decreasing trends were more significant with soil depth increase in domain north of 35°N arid and semiarid regions; in the global warming background, the simulated SM of summer demonstrated different responses to the precipitation variation. SM decreased in typical arid and semiarid regions, while SM increased in humid region. The variation distribution of SM and measured precipitation had consistencies. The humid region significant responded to precipitation, and the correlation coefficient was 0.47. While the semiarid and arid regions were ranked second.

This study showed that CLM4.0 driven by Princeton forcing data is potential in characterizing the spatial distribution and temporal spatial variation of SM in China, but the simulated SM had large systematic biases. This was relevant to land data, quality of forcing data, imperfect physical processes, and so forth. At the same time, intercomparison between measured and simulated SM at each depth and geographical location has inconsistency. All of these may cause simulation bias. So our future investigation will highly account for the high quality land and forcing data; the physical process of SM transport and parameterization of hydrological scheme will be further explored. Realistic initial states for the SM variables are required from many applications and from forecasts of weather and seasonal climate variations to models of plant growth and carbon fluxes.

Conflict of Interests

The authors declare that there is no conflict of interests regarding the publication of this paper.

Acknowledgments

This study is supported by the China Special Fund for Meteorological Research in the Public Interest (Major projects)

(Grant no. GYHY201506001-6), National Science Foundation of China (Grant nos. 41375022, 41275079, 41305077, and 41405069), Key Research Program of the Chinese Academy of Sciences (Grant no. KZZD-EW-13), and Research fund of Chengdu University of Information Technology (Grant nos. J201516 and J201518). The authors would like to thank Zhao Guohui in Cold and Arid Regions Environmental and Engineering Research Institute of Chinese Academy of Sciences. The authors also would like to thank all reviewers for their constructive comments.

References

[1] M. X. Li, Z. G. Ma, and G.-Y. Niu, "Modeling spatial and temporal variations in soil moisture in China," *Chinese Science Bulletin*, vol. 56, no. 17, pp. 1809–1820, 2011.

[2] S. I. Seneviratne, T. Corti, E. L. Davin et al., "Investigating soil moisture-climate interactions in a changing climate: a review," *Earth-Science Reviews*, vol. 99, no. 3-4, pp. 125–161, 2010.

[3] W. Dorigo, P. van Oevelen, W. Wagner et al., "A new international network for in situ soil moisture data," *Eos*, vol. 92, no. 17, pp. 141–142, 2011.

[4] W. A. Dorigo, W. Wagner, R. Hohensinn et al., "The International Soil Moisture Network: a data hosting facility for global in situ soil moisture measurements," *Hydrology and Earth System Sciences*, vol. 15, no. 5, pp. 1675–1698, 2011.

[5] W. A. Dorigo, A. Xaver, M. Vreugdenhil et al., "Global automated quality control of in situ soil moisture data from the International Soil Moisture Network," *Vadose Zone Journal*, vol. 12, no. 3, 2013.

[6] A. Wang and X. B. Zeng, "Sensitivities of terrestrial water cycle simulations to the variations of precipitation and air temperature in China," *Journal of Geophysical Research D: Atmospheres*, vol. 116, 2011.

[7] G. Balsamo, C. Albergel, A. Beljaars et al., "ERA-Interim/Land: a global land surface reanalysis data set," *Hydrology and Earth System Sciences*, vol. 19, no. 1, pp. 389–407, 2015.

[8] M. Rodell, P. R. Houser, U. Jambor et al., "The global land data assimilation system," *Bulletin of the American Meteorological Society*, vol. 85, no. 3, pp. 381–394, 2004.

[9] R. H. Reichle, "The MERRA-land data product," GMAO Office Note 3, Global Modeling and Assimilation Office, 2012, http://gmao.gsfc.nasa.gov/pubs/docs/Reichle541.pdf.

[10] T. T. Qian, A. G. Dai, K. E. Trenberth, and K. W. Oleson, "Simulation of global land surface conditions from 1948 to 2004. Part I: forcing data and evaluations," *Journal of Hydrometeorology*, vol. 7, no. 5, pp. 953–975, 2006.

[11] S. L. Guo, J. Guo, J. Zhang, and C. Hua, "VIC distributed hydrological model to predict climate change impact in the Hanjiang basin," *Science in China, Series E: Technological Sciences*, vol. 52, no. 11, pp. 3234–3239, 2009.

[12] X. Liang, D. P. Lettenmaier, E. F. Wood, and S. J. Burges, "A simple hydrologically based model of land surface water and energy fluxes for GSMs," *Journal of Geophysical Research: Atmospheres*, vol. 99, no. D7, pp. 14,415–14,428, 1994.

[13] B. Decharme, C. Ottlé, S. Saux-Picart et al., "A new land surface hydrology within the Noah-WRF land-atmosphere mesoscale model applied to semiarid environment: evaluation over the dantiandou kori (Niger)," *Advances in Meteorology*, vol. 2009, Article ID 731874, 13 pages, 2009.

[14] D. P. Dee, S. M. Uppala, A. J. Simmons et al., "The ERA-Interim reanalysis: configuration and performance of the data assimilation system," *Quarterly Journal of the Royal Meteorological Society*, vol. 137, no. 656, pp. 553–597, 2011.

[15] M. M. Rienecker, M. J. Suarez, R. Gelaro et al., "MERRA: NASA's modern-era retrospective analysis for research and applications," *Journal of Climate*, vol. 24, no. 14, pp. 3624–3648, 2011.

[16] C. Albergel, P. de Rosnay, C. Gruhier et al., "Evaluation of remotely sensed and modelled soil moisture products using global ground-based in situ observations," *Remote Sensing of Environment*, vol. 118, pp. 215–226, 2012.

[17] C. Albergel, W. Dorigo, R. H. Reichle et al., "Skill and global trend analysis of soil moisture from reanalyses and microwave remote sensing," *Journal of Hydrometeorology*, vol. 14, no. 4, pp. 1259–1277, 2013.

[18] M. Owe, R. de Jeu, and T. Holmes, "Multisensor historical climatology of satellite-derived global land surface moisture," *Journal of Geophysical Research F: Earth Surface*, vol. 113, no. 1, Article ID F01002, 2008.

[19] E. G. Njoku, T. J. Jackson, V. Lakshmi, T. K. Chan, and S. V. Nghiem, "Soil moisture retrieval from AMSR-E," *IEEE Transactions on Geoscience and Remote Sensing*, vol. 41, no. 2, pp. 215–229, 2003.

[20] Z. Bartalis, W. Wagner, V. Naeimi et al., "Initial soil moisture retrievals from the METOP-A Advanced Scatterometer (ASCAT)," *Geophysical Research Letters*, vol. 34, no. 20, Article ID L20401, 2007.

[21] L. Li, P. W. Gaiser, B.-C. Gao et al., "WindSat global soil moisture retrieval and validation," *IEEE Transactions on Geoscience and Remote Sensing*, vol. 48, no. 5, pp. 2224–2241, 2010.

[22] R. M. Parinussa, T. R. H. Holmes, and R. A. M. de Jeu, "Soil moisture retrievals from the windSat spaceborne polarimetric microwave radiometer," *IEEE Transactions on Geoscience and Remote Sensing*, vol. 50, no. 7, pp. 2683–2694, 2012.

[23] Y. H. Kerr, P. Waldteufel, J.-P. Wigneron et al., "The SMOS mission: new tool for monitoring key elements of the global water cycle," *Proceedings of the IEEE*, vol. 98, no. 5, pp. 666–687, 2010.

[24] S. Mecklenburg, M. Drusch, Y. H. Kerr et al., "ESA's soil moisture and ocean salinity mission: mission performance and operations," *IEEE Transactions on Geoscience and Remote Sensing*, vol. 50, no. 5, pp. 1354–1366, 2012.

[25] W. Dorigo, R. de Jeu, D. Chung et al., "Evaluating global trends (1988—2010) in harmonized multi-satellite surface soil moisture," *Geophysical Research Letters*, vol. 39, no. 17, Article ID L18405, 2012.

[26] Y. Y. Liu, W. A. Dorigo, R. M. Parinussa et al., "Trend-preserving blending of passive and active microwave soil moisture retrievals," *Remote Sensing of Environment*, vol. 123, pp. 280–297, 2012.

[27] Y. Y. Liu, R. M. Parinussa, W. A. Dorigo et al., "Developing an improved soil moisture dataset by blending passive and active microwave satellite-based retrievals," *Hydrology and Earth System Sciences*, vol. 15, no. 2, pp. 425–436, 2011.

[28] W. Wagner, W. Dorigo, R. de Jeu et al., "Fusion of active and passive microwave observations to create an Essential Climate Variable data record on soil moisture," in *Proceedings of the 22nd ISPRS Congress*, Melbourne, Australia, 2012.

[29] R. E. Dickinson, K. W. Oleson, G. Bonan et al., "The community land model and its climate statistics as a component of the

community climate system model," *Journal of Climate*, vol. 19, no. 11, pp. 2302–2324, 2006.

[30] K. W. Oleson, G.-Y. Niu, Z.-L. Yang et al., "Improvements to the community land model and their impact on the hydrological cycle," *Journal of Geophysical Research G: Biogeosciences*, vol. 113, no. 1, Article ID G01021, 2008.

[31] M. Decker and X. Zeng, "Impact of modified Richards equation on global soil moisture simulation in the community land model (CLM3.5)," *Journal of Advances in Modeling Earth Systems*, 2009.

[32] X. Zeng and M. Decker, "Improving the numerical solution of soil moisture-based Richards equation for land models with a deep or shallow water table," *Journal of Hydrometeorology*, vol. 10, no. 1, pp. 308–319, 2009.

[33] K. Sakaguchi and X. Zeng, "Effects of soil wetness, plant litter, and under-canopy atmospheric stability on ground evaporation in the Community Land Model (CLM3.5)," *Journal of Geophysical Research D: Atmospheres*, vol. 114, no. 1, Article ID D01107, 2009.

[34] M. G. Flanner and C. S. Zender, "Snowpack radiative heating: influence on Tibetan Plateau climate," *Geophysical Research Letters*, vol. 32, no. 6, pp. 1–5, 2005.

[35] M. G. Flanner and C. S. Zender, "Linking snowpack microphysics and albedo evolution," *Journal of Geophysical Research D: Atmospheres*, vol. 111, no. 12, 2006.

[36] M. G. Flanner, C. S. Zender, J. T. Randerson, and P. J. Rasch, "Present-day climate forcing and response from black carbon in snow," *Journal of Geophysical Research D: Atmospheres*, vol. 112, no. 11, Article ID D11202, 2007.

[37] D. M. Lawrence, A. G. Slater, V. E. Romanovsky, and D. J. Nicolsky, "Sensitivity of a model projection of near-surface permafrost degradation to soil column depth and representation of soil organic matter," *Journal of Geophysical Research F: Earth Surface*, vol. 113, no. 2, Article ID F02011, 2008.

[38] K. W. Oleson, G. B. Bonan, J. Feddema, and M. Vertenstein, "An urban parameterization for a global climate model. 1. Formulation and evaluation for two cities," *Journal of Applied Meteorology and Climatology*, vol. 47, pp. 1038–1060, 2008.

[39] N. Ramankutty, A. T. Evan, C. Monfreda, and J. A. Foley, "Farming the planet: 1. Geographic distribution of global agricultural lands in the year 2000," *Global Biogeochemical Cycles*, vol. 22, no. 1, Article ID GB1003, 2008.

[40] G. P. Asner, C. A. Wessman, D. S. Schimel, and S. Archer, "Variability in leaf and litter optical properties: Implications for BRDF model inversions using AVHRR, MODIS, and MISR," *Remote Sensing of Environment*, vol. 63, no. 3, pp. 243–257, 1998.

[41] J. Sheffield, G. Goteti, and E. F. Wood, "Development of a 50-year high-resolution global dataset of meteorological forcings for land surface modeling," *Journal of Climate*, vol. 19, no. 13, pp. 3088–3111, 2006.

[42] E. Kalnay, M. Kanamitsu, R. Kistler et al., "The NCEP/NCAR 40-year reanalysis project," *Bulletin of the American Meteorological Society*, vol. 77, no. 3, pp. 437–471, 1996.

[43] J. Sheffield and E. F. Wood, "Characteristics of global and regional drought, 1950–2000: analysis of soil moisture data from off-line simulation of the terrestrial hydrologic cycle," *Journal of Geophysical Research D: Atmospheres*, vol. 112, no. 17, 2007.

[44] J. Sheffield, K. M. Andreadis, E. F. Wood, and D. P. Lettenmaier, "Global and continental drought in the second half of the twentieth century: severity-area-duration analysis and temporal variability of large-scale events," *Journal of Climate*, vol. 22, no. 8, pp. 1962–1981, 2009.

[45] H. B. Li, A. Robock, S. X. Liu, X. G. Mo, and P. Viterbo, "Evaluation of reanalysis soil moisture simulations using updated Chinese soil moisture observations," *Journal of Hydrometeorology*, vol. 6, no. 2, pp. 180–193, 2005.

[46] S. Levis, C. Wiedinmyer, G. B. Bonan, and A. Guenther, "Simulating biogenic volatile organic compound emissions in the Community Climate System Model," *Journal of Geophysical Research D: Atmospheres*, vol. 108, no. 21, p. 4659, 2003.

[47] S. H. Suranjana, S. Moorthi, H. L. Pan et al., "The NCEP climate forecast system reanalysis," *Bulletin of the American Meteorological Society*, vol. 91, no. 8, pp. 1015–1057, 2010.

[48] A. Loew, T. Stacke, W. Dorigo, R. de Jeu, and S. Hagemann, "Potential and limitations of multidecadal satellite soil moisture observations for selected climate model evaluation studies," *Hydrology and Earth System Sciences*, vol. 17, no. 9, pp. 3523–3542, 2013.

[49] S. Nie, Y. Luo, and J. Zhu, "Trends and scales of observed soil moisture variations in China," *Advances in Atmospheric Sciences*, vol. 25, no. 1, pp. 43–58, 2008.

[50] P. Zhai, X. Zhang, H. Wan, and X. Pan, "Trends in total precipitation and frequency of daily precipitation extremes over China," *Journal of Climate*, vol. 18, no. 7, pp. 1096–1108, 2005.

[51] Y. Z. Luo, Z. G. Wang, X. M. Liu, and M. H. Zhang, "Spatial and temporal variability of precipitation in Haihe River Basin, China: characterization and management implications," *Advances in Meteorology*, vol. 2014, Article ID 143246, 9 pages, 2014.

[52] W. Shangguan, Y. Dai, B. Liu et al., "A China data set of soil properties for land surface modeling," *Journal of Advances in Modeling Earth Systems*, 2013.

[53] J. S. Famiglietti, D. Ryu, A. A. Berg, M. Rodell, and T. J. Jackson, "Field observations of soil moisture variability across scales," *Water Resources Research*, vol. 44, no. 1, Article ID W01423, 2008.

[54] C. Albergel, P. de Rosnay, G. Balsamo, L. Isaksen, and J. Muñoz-Sabater, "Soil moisture analyses at ECMWF: evaluation using global ground-based in situ observations," *Journal of Hydrometeorology*, vol. 13, no. 5, pp. 1442–1460, 2012.

[55] J. A. Saleem and G. D. Salvucci, "Comparison of soil wetness indices for inducing functional similarity of hydrologic response across sites in Illinois," *Journal of Hydrometeorology*, vol. 3, no. 1, pp. 80–91, 2002.

[56] W. A. Dorigo, W. Wagner, R. Hohensinn et al., "The international soil moisture network: a data hosting facility for global in situ soil moisture measurements," *Hydrology and Earth System Sciences*, vol. 15, pp. 1675–1698, 2011.

[57] R. D. Koster, Z. Guo, R. Yang, P. A. Dirmeyer, K. Mitchell, and M. J. Puma, "On the nature of soil moisture in land surface models," *Journal of Climate*, vol. 22, no. 16, pp. 4322–4335, 2009.